Geology
2021, Volume 49, Issue 7, Pages 799-803
https://doi.org/10.1130/G48580.1
https://archimer.ifremer.fr/doc/00686/79834/

Ice-sheet melt drove methane emissions in the Arctic during the last two interglacials

Dessandier Pierre-Antoine [1, 2, *] , Knies J. [1, 3], Plaza-Faverola A. [1], Labrousse C. [4], Renoult M. [5], Panieri G. [1]

[1] Centre for Arctic Gas Hydrate, Environment and Climate (CAGE), Department of Geosciences, The Arctic University of Norway, 9019 Tromsø, Norway
[2] L'Institut Français de Recherche pour l'Exploitation de la Mer (IFREMER)–Centre de Bretagne, Laboratoire Environnement Profond, F-29280 Plouzané, France
[3] Geological Survey of Norway, 7040 Trondheim, Norway
[4] Centre de Formation et de Recherche sur les Environnements Méditerranéens, UMR 5110, Université Via Domitia, 52 Avenue Paul Alduy, 66860 Perpignan, France
[5] Department of Meteorology, Bolin Centre for Climate Research, Stockholm University, SE-106 91 Stockholm, Sweden

* Corresponding author : Pierre-Antoine Dessandier, email address : pa.dessandier@gmail.com

Abstract :

Circum-Arctic glacial ice is melting in an unprecedented mode, and release of currently trapped geological methane may act as a positive feedback on ice-sheet retreat during global warming. Evidence for methane release during the penultimate (Eemian, ca. 125 ka) interglacial, a period with less glacial sea ice and higher temperatures than today, is currently absent. Here, we argue that based on foraminiferal isotope studies on drill holes from offshore Svalbard, Norway, methane leakage occurred upon the abrupt Eurasian ice-sheet wastage during terminations of the last (Weichselian) and penultimate (Saalian) glaciations. Progressive increase of methane emissions seems to be first recorded by depleted benthic foraminiferal δ13C. This is quickly followed by the precipitation of methane-derived authigenic carbonate as overgrowth inside and outside foraminiferal shells, characterized by heavy δ18O and depleted δ13C of both benthic and planktonic foraminifera. The similarities between the events observed over both terminations advocate for a common driver for the episodic release of geological methane stocks. Our favored model is recurrent leakage of shallow gas reservoirs below the gas hydrate stability zone along the margin of western Svalbard that can be reactivated upon initial instability of the grounded, marine-based ice sheets. Analogous to this model, with the current acceleration of the Greenland ice melt, instabilities of existing methane reservoirs below and nearby the ice sheet are likely.

INTRODUCTION

Arctic methane reservoirs consisting of gas hydrates and free gas on land and in marine sediments (> 300 m water depth) are potentially large enough to raise atmospheric methane concentrations if released during melting of glacial ice and permafrost (McGuire et al., 2009).

Although a recent analysis points towards a minor contribution of geological methane to the global carbon inventory during the last deglaciation (Dyonisius et al., 2020), very little is known about pre-Last Glacial Maximum (LGM, ca. 27-19 ka) emissions (Himmler et al., 2019). Globally, methane emissions are known to be episodic and have been linked to Quaternary sea-level changes and glacial cycles at various continental margins (Dickens et al., 1995). In the Barents Sea, the ice sheet evolution is the main driver of changes in gas hydrate stability and usually, depressurization due to the loss of subglacial loading greatly exceed hydrostatic compensation associated with relative sea level (Andreassen et al., 2017). The most prominent features are large gas blow-outs into the ocean and eventually the atmosphere that occurred upon the Svalbard-Barents Sea ice sheet (SBIS) retreat after the LGM (Andreassen et al., 2017).

Across the west-Svalbard margin regular episodic seepage started with the onset of Northern Hemisphere glaciations, ~2.7 million years ago (Ma) (Plaza-Faverola et al., 2015), with several events confirmed during the penultimate glaciation (Saalian, ca. 300-170 ka) (Himmler et al., 2019) and post LGM times (Schneider et al., 2018).

Negative $\delta^{13}C$ excursions recorded in the tests of benthic foraminifera have been used to advocate for abrupt, widespread methane seepage and oxidation through geological time (e.g., the Paleocene-Eoecene Thermal Maximum, Dickens et al., 1995). It has been shown that the precipitation of methane-derived authigenic carbonate (MDAC) overgrowth on and in foraminiferal tests explains most of the negative $\delta^{13}C$ excursions found in cold seeps (Panieri et al., 2016). Moreover, uranium-thorium - dated MDAC precipitates record past fluid flow seepage (Himmler et al., 2019), while foraminiferal MDAC are due to secondary overgrowth, either formed postsedimentation after the death of the foraminifera or synsedimentation when this process affects modern fauna (Schneider et al., 2017).

In this study, we expand the geological history of past Arctic methane release to the penultimate interglacial, the Eemian (ca. 125 ka). Based on foraminiferal $\delta^{13}C$ excursions in newly recovered boreholes, we show that Arctic methane reservoirs offshore Svalbard were not only leaking during SBIS wastage during the last deglacial cycle, but also during the Eemian (i.e. the marine isotope stage (MIS) 5e) when significantly larger ice volumes disappeared in the circum-Arctic (Jakobsson et al., 2014).

MATERIAL AND METHODS

The western Svalbard continental margin at 79°N abuts the Vestnesa Ridge, a 100 km-long sediment drift, showing flares at the ridge crest at 1200 m water depth (Bünz et al., 2012) (Fig. 1). This drift hosts a gas hydrate system with associated pockmarks and active seepage, carbonate crusts and gas hydrate at the seafloor (Panieri et al., 2017). Our results are based on drilling records of paleo-methane emissions from Vestnesa Ridge, using foraminiferal stable isotopes. $\delta^{18}O$ and $\delta^{13}C$ isotopic ratios were measured on the planktonic species *Neogloboquadrina pachyderma* and on the benthic species *Cassidulina neoteretis* supplemented by foraminiferal abundance and inorganic geochemical climate proxy parameters (Fig. 4 in the Supplemental Material[1]). One drill core (MeBo125) using the MARUM MeBo70 drill rig (Table 1, see the Supplemental Material) was collected during the *R/V Maria S. Merian* Cruise MSM57 in summer 2016 within the gas hydrate bearing “Lunde” pockmark (Fig. 1). A background site (MeBo 126) for stratigraphic correlation was drilled 1.5 km south-east of Lunde. Gravity cores (GC2 and GC3) recovered the undisturbed upper 10 m sediment sequence for each drill site (Bohrmann et al., 2016).

RESULTS AND DISCUSSION

Chronology

The stratigraphic framework for the reference GC3 core was established through correlation of $\delta^{18}O$ records with nearby sediment core HH-13-212 (Schenider et al., 2018); the latter was constrained by several accelerator mass spectrometry ^{14}C datings (Fig. 2). The glacial period is characterized by the heaviest $\delta^{18}O$ values (5 ‰) followed by a prominent meltwater injection with light $\delta^{18}O$ of ca 3.5 ‰ from the collapsing SBIS. By identifying MIS boundaries 2/1 (14 ka) and 3/2 (29 ka), both inferred from the high-resolution $\delta^{18}O$ record of GC3, a glacial sedimentation rate of ~30 cm/k.y. is estimated. These boundaries are supported by the chronology control from core HH-13-212 (Fig. 2). GC2 from the Lunde pockmark shows a similar pattern for the last glacial period, however, the initial ice-sheet collapse is followed by a prominent "shell bed" *sensu* Ambrose et al. (2015), characterized by chemosynthetic bivalves and extremely light $\delta^{13}C$ values in planktonic and benthic foraminifera (Fig. 2). MeBo 126 reference site below GC3 shows an erratic planktonic $\delta^{18}O$ record, due to incomplete sediment recovery (Bohrmann et al., 2016). Still, the characteristic carbonate preservation and high $\delta^{18}O$ values during glacial times west and north of Svalbard (Cronin et al., 2019) were here used to identify four glacial MIS stages, corresponding to the MIS 12, MIS 10, MIS 6 and MIS 2. The base of the core (62.5 m below seafloor mbsf)) has recovered the MIS 12/11 transition (~424 ka) with typical light $\delta^{18}O$ and $\delta^{13}C$ values (de Vernal and Hillaire Marcel, 2008; 60-57 mbsf) during the initial MIS 11, an interglacial characterized by an extreme warmth in the Arctic (Cronin et al., 2013) providing an average sedimentation rate of 13.9 cm ka^{-1} for the entire record. Two glacial periods (28-16.5 mbsf, 48-42.5 mbsf) with progressive increase of foraminiferal density, due to better carbonate preservation and heavy (>4.5 ‰) $\delta^{18}O$ values are identified as MIS 6 (186-130 ka) and MIS 10 (374-337 ka). Both faunal density and diversity were controlled by climate transitions, with very low abundances of the most abundant species (*C. neoteretis*) at the beginning of the glacial periods and progressive increase, in comparison with the subsequent interglacials (MIS 5, MIS 9). Calculated sedimentation rates (20 cm ka^{-1}, 15 cm ka^{-1}) for MIS 6 and MIS 10 are in the same order of magnitude as the late Weichselian (MIS 2) period (30 cm ka^{-1}). The depths of the MIS boundaries are extended to the Lunde pockmark (MeBo 125) and associated gas chimney by following undisturbed continuous reflections in high resolution 3D seismic data (Fig. 3) (Plaza-Faverola et al., 2015). The accuracy of the chrono-stratigraphic correlation between the seismic reflections and the sediment core at the MeBo reference site is within 3 m. Slightly higher uncertainties in the correlation are expected inside gas chimney structures where fracturing and unconformities challenge the continuity of the reflections (Fig. 3). Nevertheless, the consistency between the stratigraphic ages and the ages documented by Himmler et al. (2019), from dating of MDAC at the Lunde site suggest the uncertainties are not significant. Furthermore, the interval interpreted as the penultimate deglaciation in the present record is correlated with a peak of the benthic foraminiferal species *Pullenia bulloides* and a large decrease of *C. neoteretis*, both indicators for the transition MIS 6 to MIS 5e in the Arctic (Chauhan et al., 2014).

Methane Emission during the Last Deglaciation

The intense fluid seepage during the last deglaciation of the Eurasian ice sheet shows enriched $\delta^{18}O$ values, reaching 5.5 ‰ and 6 ‰ on *N. pachyderma* and *C. neoteretis*, respectively (Fig. 2), and negative excursions of $\delta^{13}C$ recorded in benthic *C. neoteretis* (-6 ‰ and -16 ‰) and planktonic *N. pachyderma* (-4 ‰ and -20 ‰) in GC2 (Fig. 2). These negative values highlight a significant impact of MDAC, as post sedimentary overgrowth, but synchronous with the establishment of the shell bed at this depth. The combination of depleted $\delta^{13}C$ and heavy $\delta^{18}O$ suggests methane release from gas hydrate dissociation, as recently observed on Vestnesa

Ridge (Dessandier et al., 2020). The main excursion (-15 to -20 ‰) corresponds to the shell bed (Fig. 3c) and is dated between 16.7 and 17.8 ka BP (Ambrose et al., 2015). Another event occurred after the final Mid-Weichselian deglaciation (650-750 cm, Fig. 3c) that corresponds to MDAC dated from the same pockmark about 43 ka (Himmler et al., 2019). These events were observed in two pockmarks (Lunde and Lomvi) in Vestnesa Ridge at similar sediment depths, documenting regional methane release during the last deglaciation, possibly driven by glacio-isostatic adjustments (Schneider et al., 2018). The dynamics of the SBIS (Patton et al., 2016) is associated with stresses due to crustal subsidence and rebound potentially affecting the properties of faults and fractures that work as conduits for fluid flow (Plaza-Faverola and Keiding, 2019). Deglaciations are characterized by rebound stress, which cause slip on faults that are close to failure due to background regional stresses (e.g., Lund, 2015). The opening of faults and fractures associated with ice-sheet dynamics has been suggested as explanation for historical methane release in the area from hydrate and free gas reservoirs (Plaza-Faverola and Keiding, 2019). Headspace data from the Lunde and Lomvi boreholes suggest a thermogenic methane origin from deep-seated carbon sources (Pape et al. 2019). The regional isotopic signals we document here are unequivocally correlated with deglaciations and support thus the notion of methane emission following the SBIS retreat.

Methane Emission during the Penultimate Interglacial, the Eemian

Analogously to the last deglaciation, the penultimate deglaciation (Termination II, ~130 ka) is characterized by negative $\delta^{13}C$ excursions in benthic foraminifera (-5 to -8 ‰) followed by concurrent strongly negative $\delta^{13}C$ signatures in both benthic and planktonic foraminifera (-8 to -20 ‰) (Fig. 3). This indicates that living benthic foraminifera incorporated ^{13}C-depleted methane-derived dissolved inorganic carbon, at the beginning of the methane emissions, before MDAC precipitation occurred (Rathburn et al., 2003). The interval at 1625 cmbsf that corresponds to the Eemian is also characterized by a shell bed (Fig. 3). All data suggest that analogous to the SBIS wastage during the last deglaciation, massive seafloor seepage also occurred during climate warming upon the end of the Saalian glaciation. Our record further suggests a progressive intensification of methane seepage from initial ice sheet retreat to full interglacial conditions. Moderate seeping phase is manifested by the initial overgrowth of foraminiferal MDAC at the MIS 6/5 transition, before intense phases of seepage allowing the formation of MDAC crusts and accumulation of chemosynthetic bivalves near the seafloor occurred in early MIS 5. These phases are correlated with abundant *C. neoteretis* (supplementary fig. 4), an indicator of Atlantic water (Wollenburg et al., 2001), which tolerates advection of methane, in contrast to *M. barleeanus*, dominant during diffusive phases (Dessandier et al., 2019). Furthermore, intense-advective phases are synchronous with foraminiferal $\delta^{18}O$ increase (Fig. 3), which has been attributed in the area to gas hydrate dissociation (Dessandier et al., 2020).

We suggest that interglacial methane emissions started upon initial ice sheet instabilities during the penultimate glacial maxima (~140 ka). Himmler et al. (2019) hypothesized that methane release on Vestnesa Ridge started because of vertical lithosphere displacements due to glacio-isostatic adjustment of the nearby ice sheet. However, this glacial stage was interrupted several times by warm water incursions (Mokeddem and McManus, 2016), causing a highly dynamic behavior of the SBIS. Hence, interactions of Atlantic-derived water masses with dynamic nearby ice sheets may have stimulated frequent ice sheet instabilities that eventually have caused leakage of deep-seated carbon sources from re-activated fault systems on a multi-centennial time scale. Emission got less intense throughout the termination until the system became stable when ice disappeared during the Eemian climate optimum (Fig. 3).

IMPLICATIONS AND CONCLUSION

The new evidence for methane release off western Svalbard suggests massive seepage during ice sheet wastage over the last (~20-15 ka) and penultimate deglaciation (~140-130 ka). The record highlights the critical effect of ice sheet melting on sub-seafloor methane reservoirs, and potentially dissociation of gas hydrates. Whether the methane release was large enough to raise its atmospheric concentration remains debated (Dyonisius et al. 2020) until more knowledge on natural methane leakage from Greenland ice core records is available. We note, however, that gas emissions on Vestnesa Ridge is not equivalent to its original old carbon source signal (Pape et al., 2019), but rather biodegraded due to microbial methane formation. More investigations are needed on this topic to explore all the controlling factors of abrupt methane emissions, including re-activation of faults and gas hydrate dissociation and biodegradation that allow methane emissions at the seafloor (Plaza-Faverola and Keiding, 2019).

However, two major emission events evidenced in this study point out the effect of ice sheet melting on sedimentary methane release during the last two glacial-interglacial cycles. We suggest that recurrent leakage of shallow gas reservoirs during climate transitions are due to recurrent instabilities of grounded, marine-based ice sheets. The Eemian interglacial has a distinct regional signature of a major methane seepage event recognized in both geological and geophysical records from northern latitudes. It may correspond thus to the best analogue for the climate of the end of the current century, with estimated similar polar warming and relative sea level (Overpeck et al., 2006). Results from this study implies that with the current acceleration of the Greenland ice melt, dissociations of existing methane reservoirs below and nearby the ice sheet are highly likely.

ACKNOWLEDGMENTS

We thank the captain and the crew of the R/V Maria S. Merian, the chief scientists G. Bohrmann and S. Bünz and are grateful to MARUM institute (Center for Marine Environmental Sciences, University of Bremen) for supporting the sampling. This study is supported by the Research Council of Norway (RCN) through its grant 287 no. 223259 and NORCRUST (#255150). PAD is supported by ISblue project (ANR-17-EURE-0015). APF contribution is in the framework of the SEAMSTRESS project supported by the Tromsø Research Foundation and the RCN (Frinatek project 287865).

REFERENCES CITED

Ambrose Jr., W.G., Panieri, G., Schneider, A., Plaza-Faverola, A., Carroll, M.L., Aström, E.K.L., Locke, V.W.L. and Carroll, J., 2015. Bivalve shell horizons in seafloor pockmarks of the last glacial interglacial transition: a thousand years of methane emissions in the Arctic Ocean. G-cubed 16, 4108e4129.https://doi.org/10.1002/2015GC005980

Andreassen, K., Hubbard, A., Winsborrow, M., Patton, H., Vadakkepuliyambatta, S., Plaza-Faverola, A., Gudlaugsson, E., Serov, P., Deryabin, A., Mattingsdal, R., Mienert, J., Bünz, S., 2017. Massive blow-out craters formed byhydrate-controlled methaneexpulsion from the Arctic seafloor. Science 356, 948-953. DOI: 10.1126/science.aal4500

Bohrmann, et al., 2016. *H.R/V MARIA S. Merian* Cruise Report MSM57—Gas Hydrate 235 Dynamics at the Continental Margin of Svalbard, Reykjavik– Longyearbyen–236 Reykjavik, 29 July–07 September 2016: University of Bremen and the Center for 237 Marine Environmental Sciences (MARUM), 205 p., http://nbn-resolving.de/urn:nbn:de:gbv:46-00105895-15

Bünz, S., Polyanov, S., Vadakkepuliyambatta, S., Consolaro, C., Mienert, J., 2012. Active gas venting through hydrate-bearing sediments on the Vestnesa Ridge, offshore W Svalbard. Marine Geology 332–334, 189–197. http://dx.doi.org/10.1016/j.margeo.2012.09.012.

Chauhan, T., Rasmussen, T.L., Noormets, R., Jakobsson, M., Hogan, K.A., 2014. Glacial history and paleoceanography of the southern Yermak Plateau since 132 ka BP. Quaternary Science Reviews 92, 155-169. https://doi.org/10.1016/j.quascirev.2013.10.023

Cronin, T., Polyak, L., Reed, D., Kandiano, E.S., Marzen, R.E., Council, E.A, 2013. A 600-ka Arctic sea-ice record from Mendeleev Ridge based on ostracodes. Quaternary Science Reviews 79, 157-167. https://doi.org/10.1016/j.quascirev.2012.12.010.

Cronin, T., Seidenstein, J., Keller, K., McDougall, K., Ruefer, A., Gemery, L., 2019. The Benthic Foraminifera Cassidulina from The Arctic Ocean: Application to Paleoceanography and Biostratigraphy. Micropaleontology 65, 105-125.

de Vernal, A. and Hillaire Marcel, C., 2008. Natural Variability of Greenland Climate, Vegetation, and Ice Volume During the Past Million Years. Science 320 (5883), 1622-1625.

Dessandier, P.-A., Borrelli, C., Kalenitchenko, D., Panieri, G., 2019. Benthic foraminifera in Arctic methane hydrate bearing sediments. Frontier in Marine Science 6:765. https://doi.org/10.3389/fmars.2019.00765

Dessandier P.-A., Panieri, G., Borrelli, C, Sauer, S., Yao, H., Hong, W.-L., 2020. Foraminiferal $\delta^{18}O$ reveals gas hydrate dissociation in Arctic Ocean sediments. Geo-marine Letters 40, 507-523. https://doi.org/10.1007/s00367-019-00635-6.

Dickens, G.R., O'Neil, J.R., Rea, D.K., Owen, R.M., 1995. Dissociation of oceanic methane hydrate as a cause of the carbon isotope excursion at the end of the Paleocene. Paleoceanography 10, 965-971. https://doi.org/10.1029/95PA02087

Dyonisius, M.N., Petrenko, V.V., Smith, A.M., Hua, Q., Yang, B., Schmitt, J., Beck, J., Seth, B., Bock, M., Hmiel, B., Vimont, I., Menking, J. A., Shackleton, S. A., Baggenstos, D., Bauska, T. K., Rhodes, R. H., Sperlich, P., Beaudette, R., Harth, C., Kalk, M., Brook, E. J., Fischer, H., Severinghaus, J.P., Weiss, R.F., 2020. Old carbon reservoirs were not important in the deglacial methane budget. Science 367 (6480), 907-910. DOI: 10.1126/science.aax0504

Goswami, B.K., Weitemeyer, K.A., Bünz, S., Minshull, T.A., Westbrook, G.K., Ker, S., Sinha, M.C., 2017. Variations in pockmark composition at the Vestnesa Ridge: Insights from marine controlled source electromagnetic and seismic data. Geochemistry, Geophysics, Geosystems 18(3), 1111-1125. https://doi.org/10.1002/2016GC006700

Himmler, T., Sahy, D., Martma, T., Bohrmann, G., Plaza-Faverola, A., Bünz, S., Condon, D.J., Knies, J., Lepland, A., 2019. A 160,000-year-old history of tectonically controlled methane seepage in the Arctic. Science Advances 5: eaaw 1450. DOI: 10.1126/sciadv.aaw1450

Jakobsson, M., Andreassen, K., Bjarnadóttir, L.R., Dove, D., Dowdeswell, J.A., England, J.H., Funder, S., Hogan, K., Ingolfsson, O., Jennings, A., Larsen, N.K., Kichne, N., Landvik, J.Y., Mayer, L., Mikkelsen, N., Möller, P., Niessen, F., Nilsson, J., O'Regan, M., Polyak, L., Nørgaard-Pedersen, N., Stein, R., 2014. Arctic Ocean glacial history. Quaternary Science Reviews 92, 40-67. https://doi.org/10.1016/j.quascirev.2013.07.033

Jessen, S.P., Rasmussen, T.L., Nielsen, T., Solheim, A., 2010. A new Late Weichselian and Holocene marine chronology for the western Svalbard slope 30,000–0 cal years BP. Quaternary Science Reviews 29, (9-10): 1301-1312. https://doi.org/10.1016/j.quascirev.2010.02.020

Lund, B., 2015. Plaeoseismology of glaciated terrain in Beer, M., et al/; eds., Encyclopedia of Earthquake Engineering: Berlin, Springer, https://doi.org/10.1007/978-3-642-36197-5_25-1

McGuire, A. D., Anderson, L.G., Christensen, T. R., Dallimore, S., Guo, L., Hayes, D.J., Heimann, M., Lorenson, T. D., MacDonald, R. W., Roulet, N., 2009. Sensitivity of the carbon cycle in the Arctic to climate change, Ecol. Monogr., 79(4), 523-555, doi:10.1890/08-2025.1

Mokeddem, Z., McManus, J.F., 2016. Persistent climatic and oceanographic oscillations in the subpolar North Atlantic during the MIS 6 glaciation and MIS 5 interglacial. Paleoceanography and Paleoclimatoogy 31(6), 758-778. https://doi.org/10.1002/2015PA002813

Overpeck, J.T., Otto-Bliesner, B.L., Miller, G.H., Muhs, D.R., Alley, R.B., Kiehl, J.T., 2006. Paleoclimatic evidence for future ice-sheet instability and rapid sea-level rise. Science 311, 1747-1750. DOI: 10.1126/science.1115159

Panieri, G., Graves, C.A., James, R.H., 2016. Paleo-methane emissions recorded in foraminifera near the landward limit of the gas hydrate stability zone off-shore western Svalbard. Geochemistry, Geophysics, Geosystem 17 (2), 521–537. http://dx.doi.org/10.1002/2015GC006153

Panieri, G., Bünz, S., Fornari, D.J., Escartin, J., Serov. P., Jansson, P., Torres, M.E., Johnson, J.E., Hong, W.L., Sauer, S., Garcia, R., Gracias, N., 2017. An integrated view of the methane system in the pockmarks at Vestnesa Ridge, 79°N. Marine Geology 390, 282-300. http://dx.doi.org/10.1016/j.margeo.2017.06.006.

Patton, H., Hubbard, A., Anrdeassen, K., Winsborrow, M., Stroeven, A.P., 2016. The build-up, configuration, and dynamical sensitivity of the Eurasian ice-sheet complex to Late Weichselian climatic and oceanic forcing. Quaternary Science Reviews 153, 97-121. https://doi.org/10.1016/j.quascirev.2016.10.009

Pape, T., Bünz, S., Hong, W.-L., Torres, M.E., Riedel, M., Panieri, G., Lepland, A., Hsu, C.-W., Wintersteller, P., Wallmann, K., Schmidt, C., Yao, H., Bohrmann, G., 2019. Origin and Transformation of Light Hydrocarbons Ascending at an Active Pockmark on Vestnesa Ridge, Arctic Ocean. Journal of Geophysical Research: Solid Earth 125(1), e2018JB016679. https://doi.org/10.1029/2018JB016679

Plaza-Faverola, A., Keiding, M., 2019. Correlation between tectonic stress regimes and methane seepage on the western Svalbard margin. Solid Earth 10 (1), 79-94. https://doi.org/10.5194/se-10-79-2019

Plaza-Faverola, A., Bünz, S., Johnson, J.E., Chand, S., Knies, J., Mienert, J., Franek, P., 2015. Role of tectonic stress in seepage evolution along the gas hydrate-charged Vestnesa Ridge. Fram Strait Geophys. Res. Lett. 42, 733-742. http://dx.doi.org/10.1002/2014GL062474

Rathburn, A.E., Pérez, M.E., Martin, J.B., Day, S.A., Mahn, C.,Gieskes, J., Ziebis, W., Williams, D., Bahls, A., 2003. Relation-ships between the distribution and stable isotopic composition of living benthic foraminifera and cold methane seep biogeochemistry in Monterey Bay, California. Geochemistry, Geophysics, Geosystems 4 (12), 1106. https://doi.org/10.1029/2003GC000595

Schneider, A., Crémière, A., Panieri, G., Lepland, A., Knies, J., 2017. Diagenetic alteration of benthic foraminifera from a methane seep site on Vestnesa Ridge (NW Svalbard). Deep-Sea Research I 123, 22-34. http://dx.doi.org/10.1016/j.dsr.2017.03.001

Schneider, A., Panieri, G., Lepland, A., Consolaro, C., Crèmiére, A., Forwick, M., Johnson, J.E., Plaza-Faverola, A., Sauer, S., Knies, J., 2018, Arctic seafloor methane seepage at Vestnesa Ridge (NW Svalbard) since the Last Glacial Maximum. Schneider A., Diagenetically altered benthic foraminifera reveal paleo-methane seepage. Quaternary Science Reviews 193, 98-117. https://doi.org/10.1016/j.quascirev.2018.06.006

Singhroha, S., Chand, S., Bünz, S., 2019. Constraints on Gas Hydrate Distribution and Morphology in Vestnesa Ridge, Western Svalbard Margin, Using Multicomponent Ocean-Bottom Seismic Data. Journal of Geophysical Research: Solid Earth. https://doi.org/10.1029/2018JB016574

Sztybor, K. and Rasmussen, T.L., 2017. Late glacial and deglacial palaeoceanographic changes at Vestnesa Ridge, Fram Strait: Methane seep versus non-seep environments. Palaeogeography, Palaeoclimatology, Palaeoecology 476, 77-89. https://doi.org/10.1016/j.palaeo.2017.04.001

Wollenburg, J.E., Kunht, W., Mackensen, A., 2001. Changes in Arctic Ocean paleoproductivity and hydrography during the last 145 kyr: The benthic foraminiferal record. Paleoceanography 16(1), 65-77. https://doi.org/10.1029/1999PA000454

Table 1. Investigated sediment cores, West Svalbard Margin

Station ID	Date dd.mm.yyyy	Latitude (°N)	Longitude (°E)	Water depth (m)	Core length (m)	Drilled length (m)
MeBo125	04.08.2016	79°00.503’	6°54.621’	1212	9.06	22.8
MeBo127	07.08.2016	79°00.418’	6°54.245’	1210	3.52	13.9
MeBo126	05.08.2016	78°59.806'	6° 57.808'	1198	24.65	62.5
GC2	03.08.2016	79°00.506	6°54.513’	1214	7.65	
GC3	03.08.2016	78°59.806'	6° 57.808'	1200	5.84	

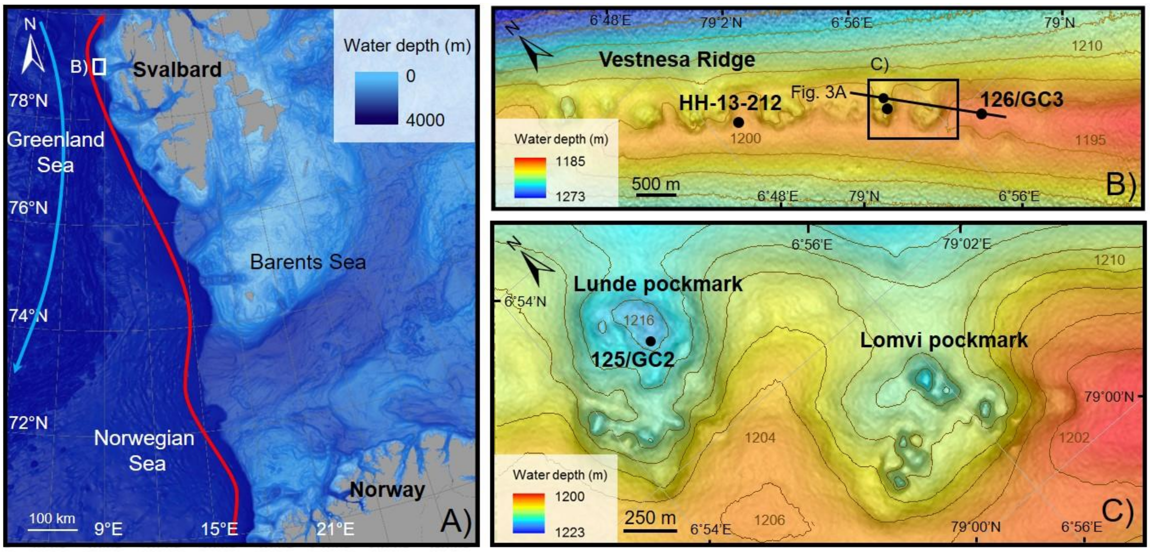

Figure 1. A) Location map of the Vestnesa Ridge, offshore Svalbard, Norway, red arrow corresponds to North Atlantic Current and blue arrow to East Greenland Current. B) Pockmarks, cores and seismic line used for chrono-stratigraphic correlation. C) Location of the studied cores.

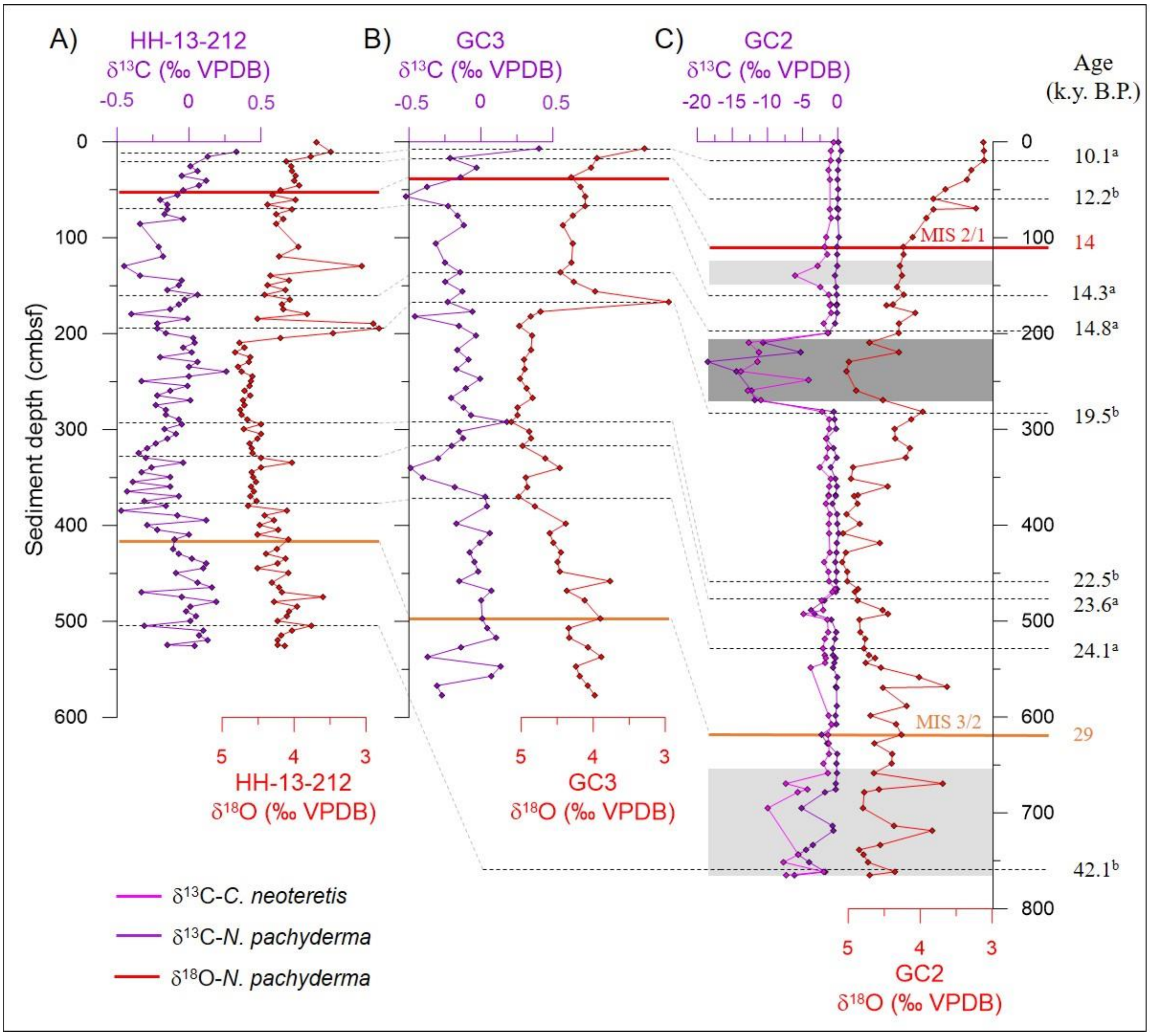

Figure 2. Foraminiferal stable isotopes (relative to Vienna Peedee belemnite (VPDB)) of the gravity core HH-13-212 from Schneider et al. (2018) and from gravity core GC3 and GC2 (this study). Grey bars represent phases of depleted $\delta^{13}C$ (light grey) and combined depleted $\delta^{13}C$ with heavy $\delta^{18}O$ (dark grey). References: a – Jessen et al. (2010) and b – Sztybor and Rasmussen (2017). MIS – marine isotope stage; cmbsf – cm below seaflorr; C. – Cassidulina; N. – Neogloboquadrina.

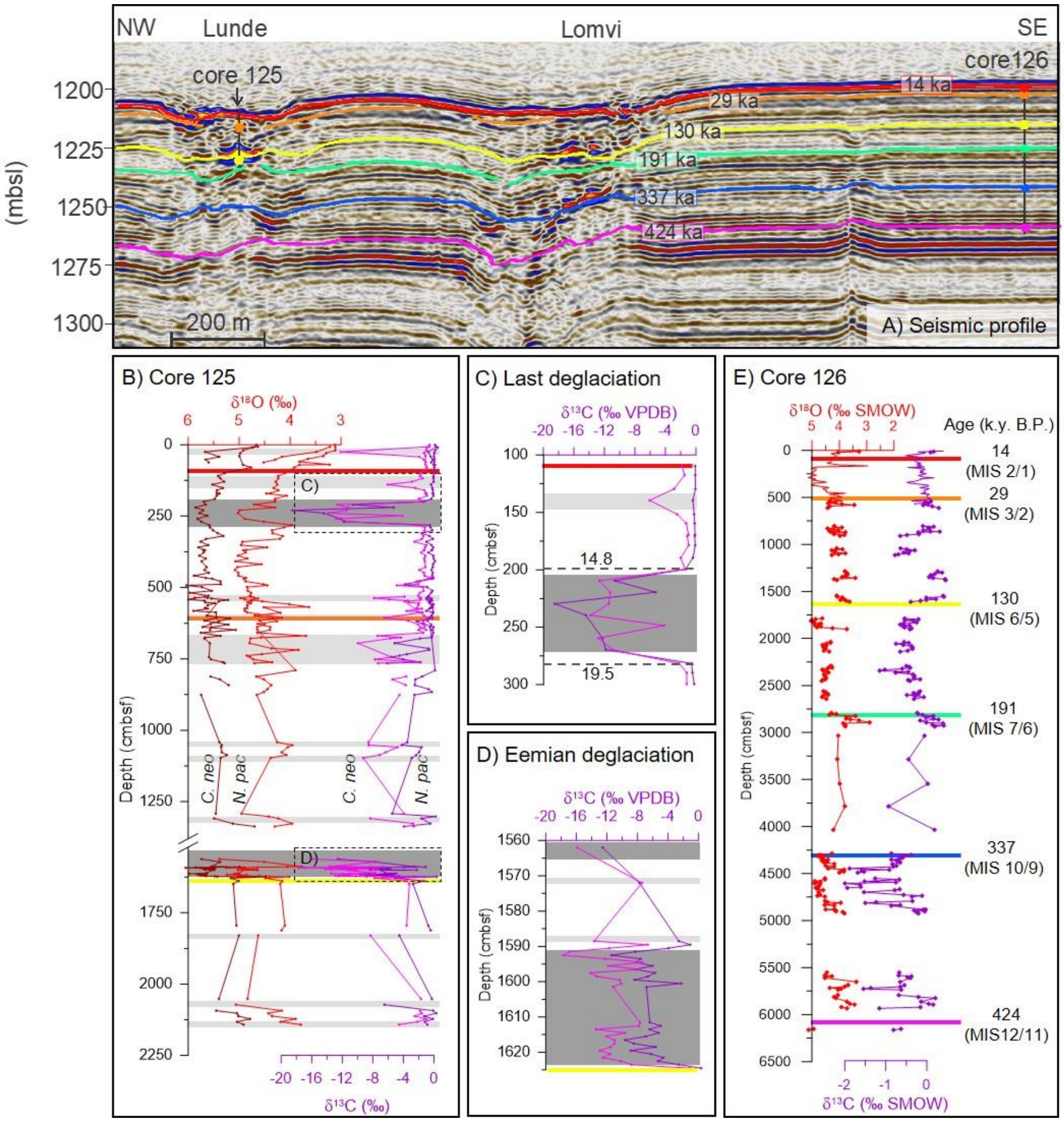

Figure 3. A) Seismic profile showing continuation of reflections between the reference site MeBo126 and site MeBo125, Svalbard, Norway. mbsl – m below sea level. B) Benthic (*C. neo* – *Cassidulina neoteretis*) and planktonic (*N. pac* – *Neogloboquadrina pachyderma*) foraminiferal stable isotopes of the cores MeBo125 and GC2 (cmbsf – cm below seafloor). C) Blow-up of the last deglaciation. VPDB – Vienna Peedee belemnite. D) Close-up of a major seepage event over the Eemian interglacial from the record of the core MeBo125. E) Planktonic foraminiferal (*N. pachyderma*) stable isotopes of the cores MeBo126 and GC3. SMOW – standard mean ocean water. Seismic profile is the transect from inline 133 in the 3D seismic volume used by Plaza-Faverola et al. (2015). Seismic data were converted to depth using P-wave velocity information from Goswami et al. (2017) and Singhroha et al. (2019). MIS – marine isotope stage.

[1]Supplemental Material (Supplementary methods on micropaleontolgy, dating and MeBo drilling and supplementary notes on chronology and foraminiferal preservation). Please visit 371 https://doi.org/10.1130/XXXXX to access the supplemental material, and contact 372 editing@geosociety.org with any questions.